

Intersection Crossing with Future-Focused Control Barrier Functions

Mitchell Black¹Mrdjan Jankovic²Abhishek Sharma²Dimitra Panagou¹

Abstract— In this paper, we introduce a future-focused control barrier function (ff-CBF) approach to an unsignaled four-way intersection crossing problem for a collection of communicating automobiles. Our novel ff-CBF encodes that vehicles take control actions that avoid predicted collisions over an arbitrarily long future time horizon, thereby defining a virtual barrier. We then propose a relaxed-virtual CBF (rv-CBF) that inherits the predictive power of the ff-CBF while allowing relaxations of the virtual barrier away from the physical barrier between vehicles. We study the efficacy of the ff-CBF and rv-CBF based controllers via a series of simulated trials of the intersection scenario and highlight how the rv-CBF based controller empirically outperforms a benchmark controller from the literature by improving intersection throughput while preserving safety and feasibility properties.

I. INTRODUCTION

Vehicles with autonomous capabilities have grown increasingly prevalent on public roadways in recent years, and growth is forecasted to continue [1]. Intersection scenarios are of keen interest due to the systemic dangers they pose; in fact, according to the U.S. Federal Highway Administration more than 50% of all fatal and injury crashes occur at intersections [2]. Some have proposed alleviating this problem by using a centralized intersection manager (IM) to communicate safe entry/exit times to incoming connected autonomous vehicles (CAVs) [3]–[5]. In contrast to schedulers, controllers offer better real-time reactivity to a dynamic, evolving environment. In the intersection setting, it is critical that control solutions are designed such that the overall system possesses both safety and liveness properties, i.e. that vehicles are able to traverse the intersection safely.

In both centralized and decentralized approaches, a common element in safe controller design is the use of control barrier functions (CBFs) [6], [7]. CBFs have been shown to be effective in compensating for some potentially unsafe control action in a variety of applications, including autonomous driving [8], robotic manipulators [9], and quadrotor control [10]. Studies have further demonstrated that CBFs are useful in maintaining safety in the presence of bounded disturbances [11] and model uncertainties [12]. To date, however, a difficulty encountered when using CBF-based approaches is their tendency to myopically focus on present safety, potentially to the detriment of future performance. This drawback can be mitigated in part by using model predictive control (MPC), which solves an optimal control problem over

a time horizon and implements the present control solution. While some recent work has demonstrated the efficacy of synthesizing CBFs with MPC frameworks for safe control [13], such controllers often require the solution to a sequence of optimization problems at a given time, where the size of each grows with the look-ahead horizon.

Motivated by these drawbacks, we introduce a new future-focused control barrier function (ff-CBF) for collision avoidance. Its fundamental underlying assumption is that the position of each vehicle evolves with constant velocity, one which we use to predict the minimum inter-agent distance over a future time interval and enforce that it remains above a safe threshold. In other words, the ff-CBF defines a zero super-level set containing vehicle states that are guaranteed to remain safe under a zero-acceleration control policy over a period of time. In this sense, control design using the ff-CBF is related to recent work on the development of backup CBF policies [14]–[16]. Unlike traditional backup policies, however, our ff-CBF does not require numerical integration of the system trajectories forward in time, the computational demands of which also grow with the look-ahead horizon. This allows us to take future safety into account while using a computationally-efficient quadratic program-based control law often used in the literature for CBF-based safe control [6], [8], [12], [17].

Predicted future safety, however, represents a *virtual* barrier which, in practice, may be violated without defying the *physical* barrier between agents. As such, we introduce the notion of a relaxed-virtual control barrier function (rv-CBF) and show that enforcing forward invariance of its zero super-level set allows permeability of the virtual barrier while satisfying the physical one. We then study the intersection crossing problem in simulation over a wide variety of initial conditions and highlight how an rv-CBF based controller provides the performance benefits of ff-CBF based control without incurring physical barrier violations.

The paper is organized as follows. Section II introduces some preliminaries, including set invariance and QP-based control. We formalize the problem under consideration in Section III and introduce our future-focused CBF in Section IV. Section V contains the results of our simulated case study, and in Section VI we conclude with final remarks and directions for future work.

II. MATHEMATICAL PRELIMINARIES

We use the following notation throughout the paper. \mathbb{R} denotes the set of real numbers. $\|\cdot\|$ represents the Euclidean norm. We write ∂S for the boundary of a closed set S , and $\text{int}(S)$ for its interior. A function, α , is said to belong

We would like to acknowledge the support of the Ford Motor Company.

¹Department of Aerospace Engineering, University of Michigan, 1320 Beal Ave., Ann Arbor, MI 48109, USA; {mblackjr, dpanagou}@umich.edu.

²Ford Research and Advanced Engineering, 2101 Village Rd., Dearborn, MI 48124, USA; {mjankov1, asharm90}@ford.com.

to extended class \mathcal{K} if $\alpha(0) = 0$ and α is increasing on the interval $(-\infty, \infty)$. The Lie derivative of a function $V : \mathbb{R}^n \rightarrow \mathbb{R}$ along a vector field $f : \mathbb{R}^n \rightarrow \mathbb{R}^n$ at a point $x \in \mathbb{R}^n$ is denoted $L_f V(x) \triangleq \frac{\partial V}{\partial x} f(x)$.

In this paper, we consider a collection of agents, \mathcal{A} , each of whose dynamics is governed by the following class of nonlinear, control-affine systems

$$\dot{\mathbf{x}}_i(t) = f(\mathbf{x}_i(t)) + g(\mathbf{x}_i(t))\mathbf{u}_i(t), \quad \mathbf{x}_i(0) = \mathbf{x}_{i0}, \quad (1)$$

where $\mathbf{x}_i \in \mathbb{R}^n$ and $\mathbf{u}_i \in \mathcal{U} \subset \mathbb{R}^m$ denote the state and control vectors respectively for agent $i \in \mathcal{A}$, and where $f : \mathbb{R}^n \rightarrow \mathbb{R}^n$ and $g : \mathbb{R}^{m \times n} \rightarrow \mathbb{R}^n$ are locally Lipschitz in their arguments and homogeneous across agents. The set \mathcal{U} denotes the set of admissible control inputs, and it is assumed that \mathcal{A} has cardinality A .

A. Forward Invariance using CBFs

Given a continuously differentiable function $h_i : \mathbb{R}^n \rightarrow \mathbb{R}$, we define a safe set S_i as

$$S_i = \{\mathbf{x}_i \in \mathbb{R}^n \mid h_i(\mathbf{x}_i) \geq 0\}, \quad (2)$$

where $\partial S_i = \{\mathbf{x}_i \in \mathbb{R}^n \mid h_i(\mathbf{x}_i) = 0\}$ and $\text{int}(S_i) = \{\mathbf{x}_i \in \mathbb{R}^n \mid h_i(\mathbf{x}_i) > 0\}$ denote the boundary and interior of S_i . The trajectories of (1) remain safe, i.e. $\mathbf{x}_i(t) \in S_i$ for all $t \geq 0$, if and only if S_i is *forward-invariant*. The following constitutes a necessary and sufficient condition for forward invariance of a set, S_i .

Lemma 1 (Nagumo's Theorem [18]). *Suppose that there exists $\mathbf{u}_i \in \mathcal{U}$ such that (1) admits a globally unique solution for each $\mathbf{x}_i(0) \in S_i$. Then, the set S_i is forward-invariant for the controlled system (1) if and only if*

$$L_f h_i(\mathbf{x}_i) + L_g h_i(\mathbf{x}_i)\mathbf{u}_i \geq 0, \quad \forall \mathbf{x}_i \in \partial S_i. \quad (3)$$

One way to render a set forward-invariant is to use CBFs in the control design.

Definition 1. [6, Definition 5] *Given a set $S_i \subset \mathbb{R}^n$ defined by (2) for a continuously differentiable function $h_i : \mathbb{R}^n \rightarrow \mathbb{R}$, the function h_i is a **control barrier function** (CBF) defined on a set D , where $S_i \subseteq D \subset \mathbb{R}^n$, if there exists an extended class \mathcal{K} function, $\alpha : \mathbb{R} \rightarrow \mathbb{R}$, such that*

$$\sup_{\mathbf{u}_i \in \mathcal{U}} [L_f h_i + L_g h_i \mathbf{u}_i] \geq -\alpha(h_i) \quad (4)$$

holds for all $\mathbf{x} \in D$.

Specifically, Definition 1 refers to a form of CBF called a *zeroing* CBF, and one that is of relative-degree¹ one with respect to the system dynamics. It is evident that (4) reduces to (3) when $\mathbf{x}_i \in \partial S_i$, thus if $h_i(\mathbf{x}(0)) \geq 0$ and h_i is a CBF then S_i is forward-invariant. For a full review of CBFs, including those of relative-degree greater than one, see [19].

¹Relative-degree is the number of times a function must be differentiated with respect to the system dynamics before the control appears explicitly.

B. Quadratic Program based Control

It has become popular to synthesize safety and stability requirements as linear constraints in a QP-based control law [6], [8]; however, QP-based controllers can also compensate for safety by deviating from some nominal input using a CBF-QP controller of the following form:

$$\begin{aligned} \mathbf{u}_i^* = \arg \min_{\mathbf{u}_i \in \mathcal{U}} \frac{1}{2} \|\mathbf{u}_i - \mathbf{u}_i^0\|^2 \\ \text{s.t.} \end{aligned} \quad (5a)$$

$$L_f h_i(\mathbf{x}_i) + L_g h_i(\mathbf{x}_i)\mathbf{u}_i \geq -\alpha(h_i(\mathbf{x}_i)), \quad (5b)$$

where \mathbf{u}_i^0 is the nominal control input. It is worth noting that (5) is guaranteed to be feasible in the absence of input constraints, i.e. when $\mathcal{U} = \mathbb{R}^m$. As will be shown in Section V, we propose a controller of the form (5) to solve the intersection crossing problem outlined in Section III.

III. PROBLEM FORMULATION

Let \mathcal{F} be an inertial frame with a point s_0 denoting its origin. Consider a collection of automobiles \mathcal{A} approaching an unsignaled four-way intersection, where the dynamics of the i^{th} vehicle are modeled as

$$\dot{x}_i = v_{r,i} (\cos \psi_i - \sin \psi_i \tan \beta_i) \quad (6a)$$

$$\dot{y}_i = v_{r,i} (\sin \psi_i + \cos \psi_i \tan \beta_i) \quad (6b)$$

$$\dot{\psi}_i = \frac{v_{r,i}}{l_r} \tan \beta_i \quad (6c)$$

$$\dot{\beta}_i = \omega_i \quad (6d)$$

$$\dot{v}_{r,i} = a_{r,i}, \quad (6e)$$

where x_i and y_i denote the position of the center of gravity (c.g.) of the vehicle with respect to s_0 , ψ_i is the orientation of the body-fixed frame, \mathcal{B}_i , with respect to \mathcal{F} , β_i is the slip angle² of the c.g. of the vehicle relative to \mathcal{B}_i (we assume $|\beta_i| < \frac{\pi}{2}$), and $v_{r,i}$ is the velocity of the rear wheel with respect to \mathcal{F} . The state of vehicle i is denoted by $\mathbf{z}_i = [x_i \ y_i \ \psi_i \ \beta_i \ v_{r,i}]^T$, and the full state is $\mathbf{z} = [\mathbf{z}_1 \dots \mathbf{z}_A]^T$. The control input is $\mathbf{u}_i = [\omega_i \ a_{r,i}]^T$, where $a_{r,i}$ is the linear acceleration of the rear wheel and ω_i the angular velocity of the slip angle, β_i , which is related to the steering angle, δ_i , via $\tan \beta_i = \frac{l_r}{l_r + l_f} \tan \delta_i$, where $l_f + l_r$ is the wheelbase with l_f (resp. l_r) the distance from the c.g. to the center of the front (resp. rear) wheel. We note that what we refer to throughout the paper as the zero-acceleration control policy, $\hat{\mathbf{u}}_i$, is defined as $\hat{\mathbf{u}}_i = [0 \ 0]^T$. The model, a visualization of which is depicted in Figure 1, is a dynamic extension of the kinematic bicycle model described in [20, Chapter 2], and is often used for autonomous vehicles [21].

With respect to safety, we consider that each vehicle must 1) obey the road speed limit and drive only in the forward direction, 2) remain inside the road boundaries, and 3) avoid collisions with all vehicles. The satisfaction of requirement

²The slip angle is the angle between the velocity vector associated with a point in a frame and the orientation of the frame.

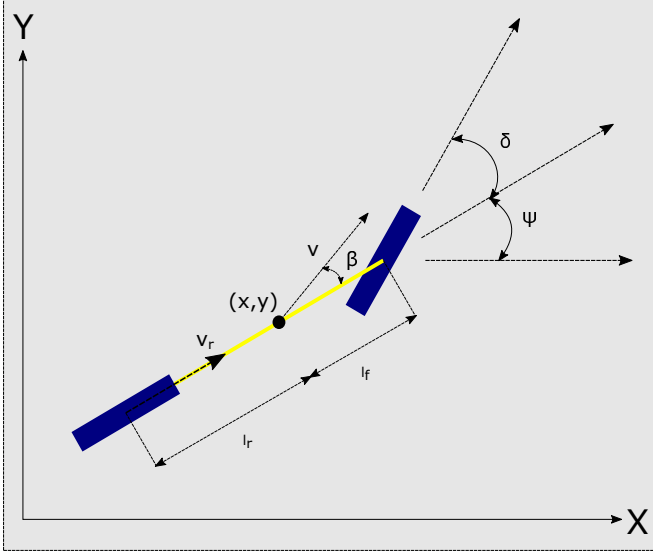


Fig. 1: Diagram of bicycle model described in (6).

2) can be handled via nominal design of ω_i , whereas we encode 1) and 3) with the following candidate CBFs:

$$h_{s,i}(\mathbf{z}_i) = (S - v_{r,i})(v_{r,i}) \quad (7)$$

$$h_{0,ij}(\mathbf{z}_i, \mathbf{z}_j) = (x_i - x_j)^2 + (y_i - y_j)^2 - (2R)^2, \quad (8)$$

where S denotes the speed limit in m/s and R is a safe radius in m. We note that (8) is widely used in the literature to encode inter-agent safety [22], [23]. Now, $h_{s,i}$ and $h_{0,ij}$ define the following safe sets at time t : $S_{s,i}(t) = \{\mathbf{z}_i(t) : h_{s,i}(\mathbf{z}_i(t)) \geq 0\}$ and $S_{0,ij}(t) = \{(\mathbf{z}_i(t), \mathbf{z}_j(t)) : h_{0,ij}(\mathbf{z}_i(t), \mathbf{z}_j(t)) \geq 0\}$, the intersection of which constitutes the safe set for a given vehicle, i.e.

$$S_i(t) = \{S_{s,i}(t) \cap S_{0,ij}(t)\}, \quad (9)$$

$$\text{where } S_{0,i}(t) = \bigcap_{j=1, j \neq i}^N S_{0,ij}(t).$$

Before introducing the problem under consideration, we introduce an assumption on the initial conditions of the vehicles.

Assumption 1. Let $0 < \bar{\tau} < \infty$. For all vehicles $i \in \mathcal{A}$ with dynamics governed by (6), the predicted closed-loop trajectories $\hat{\mathbf{z}}_i(\tau)$ over the initial time interval $[0, \bar{\tau}]$ remain safe under the zero-acceleration control policy $\hat{\mathbf{u}}_i(\tau)$, i.e. $\hat{\mathbf{z}}_i(\tau) \in S_i(\tau)$ for all $\tau \in [0, \bar{\tau}]$ under $\hat{\mathbf{u}}_i(\tau)$.

Problem 1. Consider a four-way unsignalized intersection and a set of vehicles ($i \in \mathcal{A}$) whose dynamics are described by (6). Given Assumption 1, design a control law, $\mathbf{u}_i^*(t) = [\omega_i^*(t) \ a_{r,i}^*(t)]^T$, such that, $\forall i \in \mathcal{A}$,

- i) the closed-loop trajectories remain safe for all time ($\mathbf{z}_i(t) \in S_i(t)$, $\forall t \geq 0$), and
- ii) the predicted closed-loop trajectories, $\hat{\mathbf{z}}_i(\tau)$, remain safe for all future time within a time interval $[t, t + \bar{\tau}]$ under the zero-acceleration control policy $\hat{\mathbf{u}}_i(\tau)$, i.e. $\hat{\mathbf{z}}_i(\tau) \in S_i(\tau)$, $\forall \tau \in [t, t + \bar{\tau}]$, $\forall t \geq 0$ under $\hat{\mathbf{u}}_i(\tau)$.

The presence of $\bar{\tau}$ in Assumption 1 affects the set of allowable initial conditions in the following sense: given some $\bar{\tau}$ the set of admissible initial states is $\mathcal{Z}_0(\bar{\tau}) = \{\mathbf{z} \in \mathbb{R}^{An} : F(\mathbf{z}, \bar{\tau}) \geq 0\}$, where $F : \mathbb{R}^{An} \times \mathbb{R}_{\geq 0} \rightarrow \mathbb{R}$ is a function that is non-negative if $\forall i \in \mathcal{A}$, $\hat{\mathbf{z}}_i(\tau) \in S_i(\tau)$ for all $\tau \in [0, \bar{\tau}]$ under $\hat{\mathbf{u}}_i(\tau)$, and negative otherwise. Alternatively, given some initial state $\mathbf{z}(0)$, where $\forall i \in \mathcal{A}$, $\mathbf{z}_i(0) \in S_i(0)$, the allowable look-ahead horizon is $0 < \bar{\tau} < T$, where $T \in \mathbb{R}_{\geq 0}$ is the minimum value for which $F(\mathbf{z}(0), T) = 0$. If no such value exists, then T can be arbitrarily large.

In the following section, we introduce a function that both meets the criteria for F and serves as a facet of our proposed solution to Problem 1: a future-focused control barrier function (ff-CBF) suitable for QP-based controllers.

IV. MAIN RESULTS

We first recall the nominal CBF for inter-agent safety (8), and note that for two agents i and j it may be rewritten as

$$h_{0,ij}(\mathbf{z}_i, \mathbf{z}_j) = D_{ij}^2(\mathbf{z}_i, \mathbf{z}_j) - (2R)^2, \quad (10)$$

where $D_{ij}(\mathbf{z}_i, \mathbf{z}_j) = \sqrt{(x_i - x_j)^2 + (y_i - y_j)^2}$. Let the differential inter-agent position, ξ_{ij} , velocity, ν_{ij} , and acceleration, α_{ij} , vectors be

$$\begin{aligned} \xi_{ij}(t) &= [\xi_{x,ij}, \ \xi_{y,ij}]^T = [x_i - x_j, \ y_i - y_j]^T, \\ \nu_{ij}(t) &= [\nu_{x,ij}, \ \nu_{y,ij}]^T = [\dot{x}_i - \dot{x}_j, \ \dot{y}_i - \dot{y}_j]^T, \\ \alpha_{ij}(t) &= [\alpha_{x,ij}, \ \alpha_{y,ij}]^T = [\ddot{x}_i - \ddot{x}_j, \ \ddot{y}_i - \ddot{y}_j]^T, \end{aligned}$$

where we have omitted the argument t for conciseness. In what follows, we also drop the subscript ij from D , ξ , ν , and α . The critical observation is that the inter-agent distance at any arbitrary time, T , is $D(\mathbf{z}_i, \mathbf{z}_j, T) = \|\xi(T)\|$. By assuming zero acceleration, we can use a linear model to predict that at time $T = t + \tau$, we will have that $\xi(t + \tau) = \xi(t) + \nu(t)\tau$, which implies that the predicted distance at a time of $t + \tau$ is

$$D(\mathbf{z}_i, \mathbf{z}_j, t + \tau) = \sqrt{\xi_x^2 + \xi_y^2 + 2\tau(\xi_x \nu_x + \xi_y \nu_y) + \tau^2(\nu_x^2 + \nu_y^2)}.$$

Then, we may define the minimum predicted future distance between agents as

$$D(\mathbf{z}_i, \mathbf{z}_j, t + \tau^*) = \|\xi(t) + \nu(t)\tau^*\|, \quad (11)$$

where

$$\tau^* = \arg \min_{\tau \in \mathbb{R}} D^2(\mathbf{z}_i, \mathbf{z}_j, t + \tau) = -\frac{\xi_x \nu_x + \xi_y \nu_y}{\nu_x^2 + \nu_y^2}. \quad (12)$$

A. Future-Focused CBF

We now introduce our future-focused CBF for collision avoidance:

$$h_{\hat{\tau},ij}(\mathbf{z}_i, \mathbf{z}_j) = D_{ij}^2(\mathbf{z}_i, \mathbf{z}_j, t + \hat{\tau}) - (2R)^2, \quad (13)$$

where

$$\hat{\tau} = \hat{\tau}^* K_0(\hat{\tau}^*) + (\bar{\tau} - \hat{\tau}^*) K_{\bar{\tau}}(\hat{\tau}^*), \quad (14)$$

with $\bar{\tau} > 0$ representing the length of the look-ahead horizon, $K_{\delta}(s) = \frac{1}{2} + \frac{1}{2} \tanh(k(s - \delta))$, $k > 0$, and

$$\hat{\tau}^* = -\frac{\xi_x \nu_x + \xi_y \nu_y}{\nu_x^2 + \nu_y^2 + \varepsilon}, \quad (15)$$

where $0 < \varepsilon \ll 1$. Using (14) alleviates undesirable characteristics of (12), namely that τ^* may become unbounded. The inclusion of ε makes (15) well-defined, and $K_\delta(t)$ allows (14) to smoothly approximate $\hat{\tau}^*$ between 0 and $\bar{\tau}$.

It is worth mentioning that the ff-CBF is related to the backup CBFs used for safe control design in [14], [15] in the following sense: whereas our formulation seeks to ensure that vehicles preserve safety in the future under the zero-acceleration policy, \hat{u}_i , past works have required a backup policy to actively intervene, e.g. to apply proportional braking, in order to guarantee safety.

We now show that $h_{\hat{\tau},ij}$ is indeed continuously differentiable, thus solidifying it as a candidate CBF.

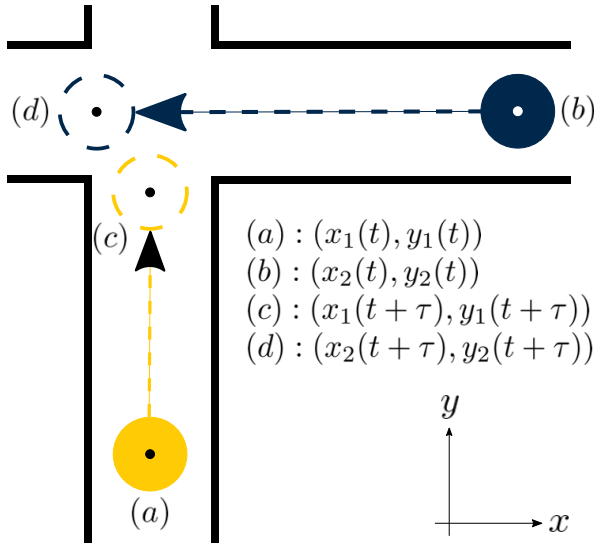


Fig. 2: Visualization of the effect of the ff-CBF. Whereas $h_{0,12}$ is evaluated based on the locations of vehicles 1 and 2 at time t , i.e. (a) and (b), $h_{\hat{\tau},12}$ evaluates safety based on the predicted future locations of the vehicles at time $t + \tau$, i.e. (c) and (d), allowing the present control to take action to avoid predicted future danger.

Theorem 1. Consider two agents governed by the dynamics (6) whose states are \mathbf{z}_i and \mathbf{z}_j . Suppose that $h_{\hat{\tau},ij}$ is defined by (13), with $\hat{\tau}$ given by (14). Then, the following hold for all bounded $\mathbf{z}_i, \mathbf{z}_j$:

- i) $h_{\hat{\tau},ij} \in \mathcal{C}^1$
- ii) $h_{\hat{\tau},ij} \leq h_{0,ij}$ whenever $\hat{\tau} \leq 2\hat{\tau}^*$

Proof. For the first part, we must show that the derivative of (13) is well-defined and continuous. Consider that from (11), (13), and (14) we have

$$\begin{aligned} \dot{h}_{\hat{\tau},ij}(\mathbf{z}) &= 2\xi_x \nu_x + 2\xi_y \nu_y + 2\dot{\hat{\tau}}(\xi_x \nu_x + \xi_y \nu_y) \\ &\quad + 2\hat{\tau}(\nu_x^2 + \nu_y^2 + \xi_x \alpha_x + \xi_y \alpha_y) \\ &\quad + 2\hat{\tau}\dot{\hat{\tau}}(\nu_x^2 + \nu_y^2) + 2\hat{\tau}^2(\nu_x \alpha_x + \nu_y \alpha_y). \end{aligned}$$

Since $\hat{\tau}$ is bounded by definition, it follows that $h_{\hat{\tau},ij} \in \mathcal{C}^1$ when $\hat{\tau} \in \mathcal{C}^1$. From (14), we have

$$\dot{\hat{\tau}} = \dot{\hat{\tau}}^*(K_0(\hat{\tau}^*) - K_{\bar{\tau}}(\hat{\tau}^*)) + \hat{\tau}^*(\dot{K}_0(\hat{\tau}^*) - \dot{K}_{\bar{\tau}}(\hat{\tau}^*)),$$

where

$$\dot{K}_\delta(\hat{\tau}^*) = \dot{\hat{\tau}}^* \frac{k}{2} \operatorname{sech}^2(k(\hat{\tau}^* - \delta))$$

and from (15)

$$\dot{\hat{\tau}}^* = -\frac{\alpha_x(2\nu_x \tau^* + \xi_x) + \alpha_y(2\nu_y \tau^* + \xi_y) + \nu_x^2 + \nu_y^2}{\nu_x^2 + \nu_y^2 + \varepsilon}$$

since $\dot{\hat{\tau}}^*$ and $\dot{K}_\delta(t)$ are bounded and continuous for bounded arguments, we have that $\hat{\tau} \in \mathcal{C}^1$ for bounded $\mathbf{z}_i, \mathbf{z}_j$. Thus, $h_{\hat{\tau},ij} \in \mathcal{C}^1$.

For the second part, we observe that $h_{\hat{\tau},ij}(\mathbf{z}) = h_{0,ij}(\mathbf{z}) + 2\hat{\tau}(\xi_x \nu_x + \xi_y \nu_y) + \hat{\tau}^2(\nu_x^2 + \nu_y^2)$, thus $h_{\hat{\tau},ij}(\mathbf{z}_i, \mathbf{z}_j) \leq h_{0,ij}(\mathbf{z}_i, \mathbf{z}_j)$ whenever

$$\hat{\tau} \leq -2 \frac{\xi_x \nu_x + \xi_y \nu_y}{\nu_x^2 + \nu_y^2} = 2\tau^*. \quad (16)$$

With ε in the denominator of (15), it follows that $\hat{\tau}^* < \tau^*$ whenever $\tau^* > 0$ (and $\hat{\tau}^* = 0$ when $\tau^* = 0$), thus (16) holds whenever $\hat{\tau} \leq 2\hat{\tau}^*$. It follows, then, that $h_{\hat{\tau},ij}(\mathbf{z}) \leq h_{0,ij}(\mathbf{z})$ whenever $\hat{\tau} \leq 2\hat{\tau}^*$. \square

Remark 1. Since $h_{\hat{\tau},ij} \in \mathcal{C}^1$, we have by Definition 1 that if there exists an extended class \mathcal{K} function, $\alpha(\cdot)$, such that (4) holds, then $h_{\hat{\tau},ij}$ is a valid CBF.

Remark 2. The condition $\hat{\tau} \leq 2\hat{\tau}^*$ may be satisfied $\forall \hat{\tau}^* \geq 0$ via sufficiently large choice of k in $K_\delta(t)$. In our simulations, we have found that $k > 10$ works well.

It is important to note that the zero level set defined by candidate CBF $h_{\hat{\tau},ij}$ represents a *virtual barrier*. Specifically, $h_{\hat{\tau},ij}(\mathbf{z}_i, \mathbf{z}_j) < 0$ does not imply that $h_{0,ij}(\mathbf{z}_i, \mathbf{z}_j) < 0$, nor does it suggest that a collision is unavoidable; rather, $h_{\hat{\tau},ij}(\mathbf{z}_i, \mathbf{z}_j) < 0$ suggests that a future collision will occur if the zero-acceleration control policy, \hat{u}_k , is applied uniformly by each vehicle $k \in \{i, j\}$. In this sense, it is conservative. This motivates the notion of the relaxed-virtual control barrier function (rv-CBF).

B. Relaxed Virtual Safety

For the above reasons, (13) represents a soft constraint, a *virtual CBF*. It is the safe set defined by the *physical CBF* (10) that must be rendered forward-invariant to guarantee collision avoidance among vehicles. This motivates the notion of a relaxed-virtual safe set,

$$S_{H,ij} = \{(\mathbf{z}_i, \mathbf{z}_j) \in \mathbb{R}^{2n} \mid H_{ij}(\mathbf{z}_i, \mathbf{z}_j) \geq 0\}, \quad (17)$$

defined implicitly by an rv-CBF:

$$H_{ij}(\mathbf{z}_i, \mathbf{z}_j) = h_{\hat{\tau},ij}(\mathbf{z}_i, \mathbf{z}_j) + \gamma(h_{0,ij}(\mathbf{z}_i, \mathbf{z}_j)), \quad (18)$$

with $\gamma : \mathbb{R} \rightarrow \mathbb{R}$ an extended class \mathcal{K} function. The following theorem shows how an rv-CBF of the form (18) renders the *physical* zero super-level set of (10) forward-invariant.

Theorem 2. Consider two agents, each of whose dynamics are described by (1). Suppose that H_{ij} is given by (18), and that $H_{ij} \geq 0$ at $t = 0$. If there exist control inputs, \mathbf{u}_i and \mathbf{u}_j , such that the following condition holds, for all $t \geq 0$,

$$\sup_{\mathbf{u}_i, \mathbf{u}_j \in \mathcal{U}} [L_{f_i} H_{ij} + L_{f_j} H_{ij} + L_{g_i} H_{ij} \mathbf{u}_i + L_{g_j} H_{ij} \mathbf{u}_j] \geq 0, \quad (19)$$

for all $\mathbf{z} \in \partial S_{H,ij}$, then, the physical safe set defined by $S_{0,ij}(t) = \{(\mathbf{z}_i, \mathbf{z}_j) \in \mathbb{R}^{2n} \mid h_{0,ij}(\mathbf{z}_i, \mathbf{z}_j) \geq 0\}$ is forward-invariant under $\mathbf{u}_i, \mathbf{u}_j$, i.e. there is no collision between agents i and j .

Proof. In order to show that $S_{0,ij}$ is rendered forward-invariant by (19), we must show that (19) implies that $\dot{h}_{0,ij} \geq 0$ whenever $h_{0,ij} = 0$. We will prove this by contradiction.

Suppose that $H_{ij}, h_{0,ij} = 0$, and that (19) holds but $\dot{h}_{0,ij} < 0$. Then, it follows that $\dot{h}_{0,ij} = 2(\xi_x \nu_x + \xi_y \nu_y) < 0$, which by (14) implies that $\hat{\tau} > 0$. With $\hat{\tau} > 0$, it follows that $h_{\hat{\tau},ij} < h_{0,ij} = 0$. However, we have assumed that $H_{ij}, h_{0,ij} = 0$, which means by definition that $h_{\hat{\tau},ij} = 0$. Thus, we have reached a contradiction. It follows, then, that (19) implies that $\dot{h}_{0,ij} \geq 0$ whenever $h_{0,ij} = 0$. As such, $S_{0,ij}$ is rendered forward-invariant. \square

Remark 3. While (18) is specific to the nominal (10) and future-focused (13) CBFs for inter-agent safety, it provides a framework for any present- and future-focused CBFs related by $h(\mathbf{x}) = h_0(\mathbf{x}) - F(\mathbf{x})$, where h_0 encodes a hard constraint, h a soft constraint, and F is some function relating the two.

As a result of Theorem 2, we can use (18) to encode safety in the context of a CBF-QP control scheme (5). In the ensuing section, we conduct a comparative study on the efficacy of the nominal (8), future-focused (13), and relaxed-virtual (18) CBFs across randomized trials of an automotive intersection crossing problem.

V. NUMERICAL CASE STUDY

In this section, we illustrate how using an rv-CBF in a centralized CBF-QP control scheme improves intersection throughput in a 4-vehicle unsignaled intersection scenario while producing promising results on safety and QP feasibility. Specifically, we study the varying degrees of success of three different centralized controllers to solve Problem 1, all of which take the following form:

$$\mathbf{u}_i^* = [\omega_i^* \ a_{r,i}^*]^T, \forall i = 1, \dots, A, \quad (20)$$

where

$$\omega_i^* = \min(\max(\omega_i^0, -\bar{\omega}), \bar{\omega}), \quad (21)$$

and

$$[a_{r,1}^* \dots a_{r,A}^*]^T = \arg \min_{[u_{12} \dots u_{A2}]} \frac{1}{2} \sum_{i=1}^A (u_{i2} - a_{r,i}^0)^2 \quad (22a)$$

$$\text{s.t. } \forall i, j = 1, \dots, A, j \neq i \\ Au_{i2} \leq b, \quad (22b)$$

$$L_f h_{s,i} + L_g h_{s,i} u_{i2} + \alpha_{s,i}(h_{s,i}) \geq 0, \quad (22c)$$

$$L_f h_{ij} + L_{g_i} h_{ij} u_{i2} + L_{g_j} h_{ij} u_{j2} + \alpha_{ij}(h_{ij}) \geq 0, \quad (22d)$$

where u_{ik} denotes the k^{th} control input of agent i , ω_i^0 and $a_{r,i}^0$ denote the nominal inputs computed using LQR (see Appendix I for a detailed explanation), (22b) encodes input constraints of the form $-\bar{a}_r \leq u_{i2} \leq \bar{a}_r$, (22c) enforces both the road speed limit and the requirement that vehicles

do not reverse, and (22d) is the inter-agent safety condition. Specifically, the three controllers under examination are (20) with 1) $h_{ij} = h_{0,ij}$ according to (10) (0-CBF), 2) $h_{ij} = h_{\hat{\tau},ij}$ from (13) (ff-CBF), and 3) $h_{ij} = H_{ij}$ via (18) (rv-CBF), with $\gamma(h_{0,ij}) = k_0 h_{0,ij}$, where $k_0 = 0.1 \max(\hat{\tau} - 1, \varepsilon)$, $\varepsilon = 0.001$, the look-ahead horizon $\hat{\tau} = 5$, and $\alpha_{ij}(h_{ij}) = 10h_{ij}$, $\bar{\omega} = \pi/2$, and $\bar{a}_r = 9.81$ for all cases. We note that (20) is centralized in the sense that is assumed that all states, \mathbf{z}_i , and nominal control inputs, \mathbf{u}_i^0 , are known.

A. Setup

For each study, we performed $N = 1000$ trials of simulated trajectories of 4 vehicles approaching the intersection from different lanes, all of whose dynamics are described by (6), using the control scheme described by (20). At the beginning of each trial, the vehicles were assigned to a lane and their initial conditions were randomized via

$$d_i = d_0 + U(-\Delta_d, \Delta_d), \\ s_i = s_0 + U(-\Delta_s, \Delta_s),$$

where d_i denotes the initial distance of vehicle i from the intersection and s_i its initial speed. We chose $d_0 = 12m$, $\Delta_d = 5m$, $s_0 = 6m/s$, and $\Delta_s = 3m/s$, and let $U(a, b)$ denote a sample from the uniform random distribution between a and b . For the speed limit, we chose $S = 10m/s$.

For performance evaluation, we introduce some metrics:

- i) Success: $\frac{\text{Number of Successful Trials}}{\text{Number of Trials}}$,
- ii) Feas.: $\frac{\text{Number of Trials in which QP is Always Feasible}}{\text{Number of Trials}}$,
- iii) DLock: $\frac{\text{Number of Trials in which Vehicles become deadlocked}}{\text{Number of Trials}}$,
- iv) Unsafe: $\frac{\text{Number of Trials Vehicles in which } h_{0,ij} < 0}{\text{Number of Trials}}$,

where a successful trial is characterized as one where all vehicles exit the intersection at their desired location, a deadlock is characterized as when all vehicles have stopped and remained stopped for 3 sec, and we define “Avg. Time” as the average time in which the final vehicle reached the intersection exit over all successful trials.

We examined the performance of each controller under two circumstances: 1) each vehicle seeks to proceed straight through the intersection without turning, and 2) three vehicles seek to proceed straight without turning and one seeks to make a left turn.

B. Results

The results for the 3 different controllers are compiled in Tables I and II respectively. Although the 0-CBF in a centralized QP-based control law is known to guarantee safety and QP feasibility under certain conditions [23], such a controller has no predictive power and is therefore prone to deadlocks. We illustrate such a deadlock in Figure 3a.

TABLE I: Controller Performance – All Proceed Straight

CBF	Success	Feas.	DLock	Unsafe	Avg. Time
$h_{ij} = h_{0,ij}$	0.653	1	0.347	0	5.67
$h_{ij} = h_{\hat{\tau},ij}$	1	1	0	0	3.45
$h_{ij} = H_{ij}$	1	1	0	0	3.21

TABLE II: Controller Performance – One Left Turn

CBF	Success	Feas.	DLock	Unsafe	Avg. Time
$h_{ij} = h_{0,ij}$	0.689	1	0.311	0	7.75
$h_{ij} = h_{\hat{\tau},ij}$	0.963	0.963	0	0	5.33
$h_{ij} = H_{ij}$	1	1	0	0	4.91

The ff-CBF-based controller succeeded as long as it was feasible, offering a 39% reduction in average time over the 0-CBF in the straight scenario and an 31% time improvement in the turning scenario, but suffered from virtual constraint violations leading to QP infeasibility in the case of turning vehicles as shown in Figure 3b. The rv-CBF controller both enjoyed the same empirical feasibility and safety as the 0-CBF design and improved the average success time to a similar extent as the ff-CBF, specifically by 43% and 36% for the straight and turning scenarios respectively. In addition, the rv-CBF control scheme achieved 100% feasibility even in the turning scenario, despite the constant velocity prediction model not taking a change of heading into account. We leave any theoretical guarantees of feasibility, however, to future work. The state, control, and rv-CBF trajectories for a turning trial are illustrated in Figures 4-6, and we provide code and a selection of videos on Github³. It can be seen from Figure 5 that the control actions smoothly take action in advance of any dangerous scenario, and from Figure 6 that both H_{ij} and $h_{0,ij}$ remain non-negative for all i, j .

VI. CONCLUSION

In this paper, we studied an intersection crossing problem for a collection of automobiles controlled by a centralized CBF-QP-based controller under three different CBFs. As a model, we selected a widely-used rear-driving dynamic bicycle model, and introduced a future-focused CBF for collision avoidance and a relaxation thereof, the relaxed-virtual CBF. We then performed a comparative numerical study on the efficacy of the centralized control scheme under the 0-CBF, ff-CBF, and rv-CBF protocols, and discovered that the rv-CBF produced the most favorable empirical results.

In the future, we plan to further investigate the following topics: 1) how the presence of non-communicating vehicles approaching the intersection affects results on safety, QP-feasibility, and throughput; 2) how we might be able to combine the predictive power of the future-focused and relaxed-virtual CBFs with control Lyapunov functions in order to make formal statements about guarantees on stabilization and safety; and 3) under what conditions the nominal CBF-based controller remains feasible when predictive CBF-based control schemes may not be.

REFERENCES

- [1] (2020, Sep) A new idc forecast shows how vehicles will gradually incorporate technologies that lead to autonomy. [Online]. Available: <https://www.idc.com/getdoc.jsp?containerId=prUS46887020>
- [2] (2021, Aug) Office of research, development, and technology at the turner-fairbank highway research center: Intersection safety. [Online]. Available: <https://highways.dot.gov/research/research-programs/safety/intersection-safety>
- [3] K. Dresner and P. Stone, “A multiagent approach to autonomous intersection management,” *Journal of artificial intelligence research*, vol. 31, pp. 591–656, 2008.
- [4] K. Yang, S. I. Guler, and M. Menendez, “Isolated intersection control for various levels of vehicle technology: Conventional, connected, and automated vehicles,” *Transportation Research Part C: Emerging Technologies*, vol. 72, pp. 109–129, 2016.
- [5] M. Khayatian, Y. Lou, M. Mehrabian, and A. Shirvastava, “Crossroads+: a time-aware approach for intersection management of connected autonomous vehicles,” *ACM Transactions on Cyber-Physical Systems*, vol. 4, no. 2, pp. 1–28, 2019.
- [6] A. D. Ames, X. Xu, J. W. Grizzle, and P. Tabuada, “Control barrier function based quadratic programs for safety critical systems,” *IEEE Trans. on Automatic Control*, vol. 62, no. 8, pp. 3861–3876, 2017.
- [7] W. Xiao, C. Belta, and C. G. Cassandras, “Decentralized merging control in traffic networks: A control barrier function approach,” in

³Link to Github repo: github.com/6lackmitchell/intersection_management

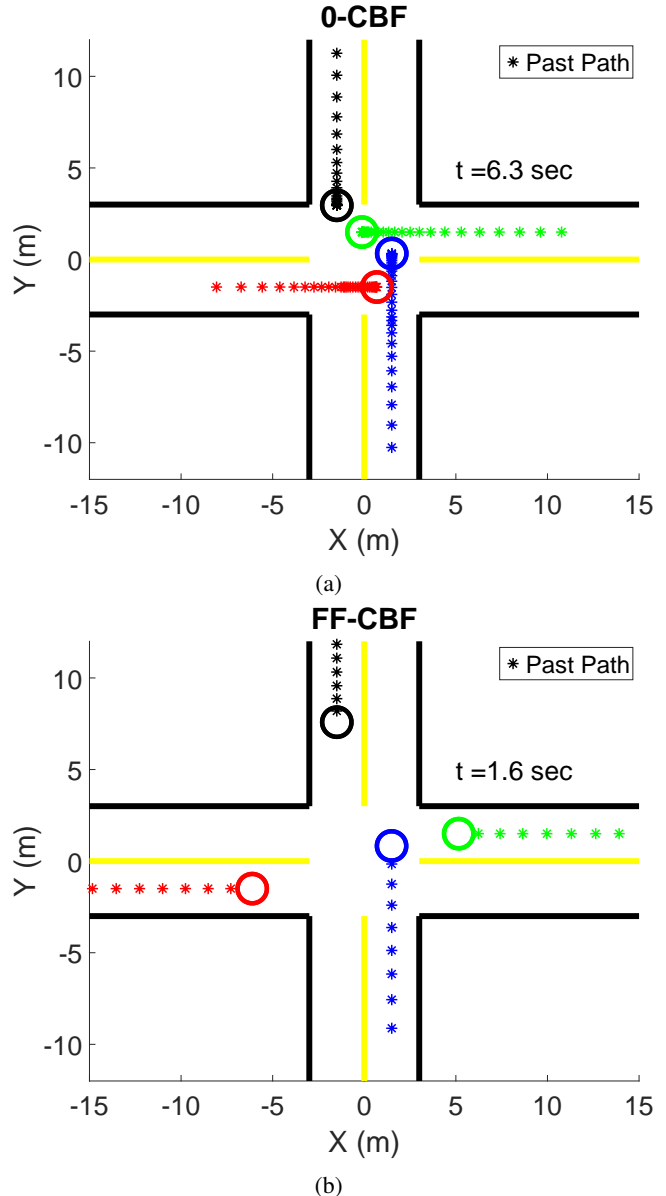


Fig. 3: Selected XY trajectories for the intersection crossing problem using (a) 0-CBF (Straight Trial 582) and (b) ff-CBF (Turning Trial 137). In (a), the centralized controller has no predictive power and the vehicles deadlock, whereas in (b) the virtual barrier between blue and black vehicles is violated as the blue vehicle begins to execute a left turn despite a wide physical margin.

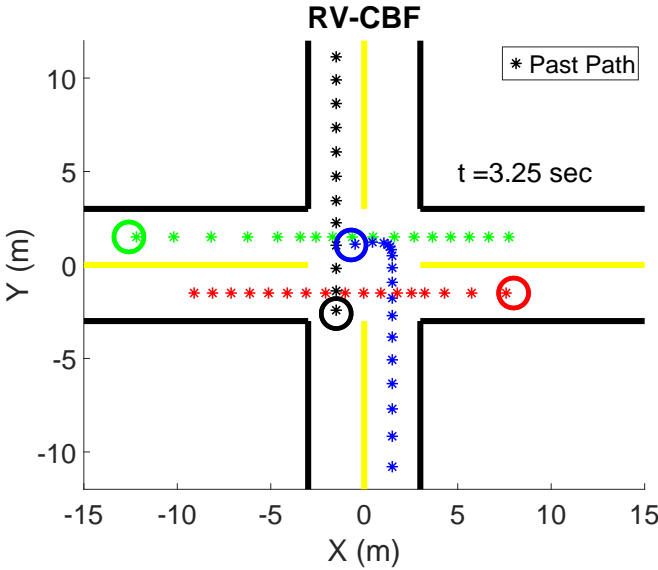


Fig. 4: XY trajectories for Trial 650 of the rv-CBF simulation set.

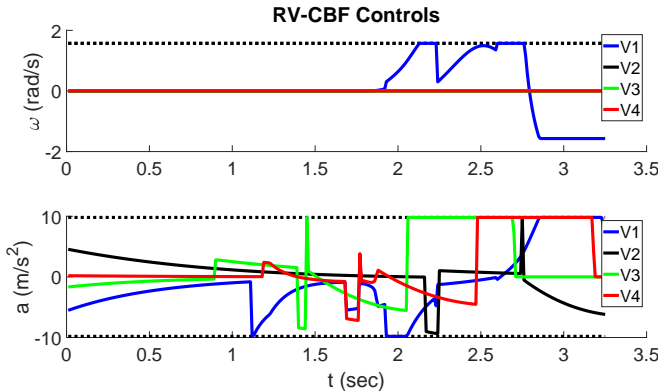


Fig. 5: Control solutions for Trial 650 of rv-CBF simulation set.

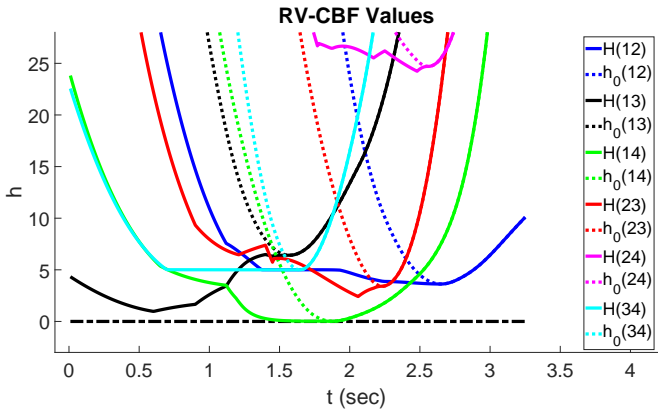


Fig. 6: rv-CBF (H) and 0-CBF (h_0) trajectories for rv-CBF Trial 650. The arguments (ij) denote that CBF is evaluated for vehicles i and j .

safety for robotic manipulators," in *2019 IEEE/RSJ International Conf. on Intelligent Robots and Systems*, 2019, pp. 173–178.

- [10] L. Wang, E. A. Theodorou, and M. Egerstedt, "Safe learning of quadrotor dynamics using barrier certificates," in *2018 IEEE International Conf. on Robotics and Automation*, 2018, pp. 2460–2465.
- [11] M. Jankovic, "Robust control barrier functions for constrained stabilization of nonlinear systems," *Automatica*, vol. 96, pp. 359–367, 2018.
- [12] M. Black, E. Arabi, and D. Panagou, "A fixed-time stable adaptation law for safety-critical control under parametric uncertainty," in *2021 European Control Conference (ECC)*, 2021, pp. 1328–1333.
- [13] J. Zeng, B. Zhang, and K. Sreenath, "Safety-critical model predictive control with discrete-time control barrier function," in *2021 American Control Conference (ACC)*, 2021, pp. 3882–3889.
- [14] T. Gurriet, M. Mote, A. Singletary, P. Nilsson, E. Feron, and A. D. Ames, "A scalable safety critical control framework for nonlinear systems," *IEEE Access*, vol. 8, pp. 187249–187275, 2020.
- [15] Y. Chen, M. Jankovic, M. Santillo, and A. D. Ames, "Backup control barrier functions: Formulation and comparative study," *arXiv preprint arXiv:2104.11332*, 2021.
- [16] A. Singletary, A. Swann, Y. Chen, and A. D. Ames, "Onboard safety guarantees for racing drones: High-speed geofencing with control barrier functions," *IEEE Robotics and Automation Letters*, vol. 7, no. 2, pp. 2897–2904, 2022.
- [17] M. Rauscher, M. Kimmel, and S. Hirche, "Constrained robot control using control barrier functions," in *IEEE/RSJ International Conference on Intelligent Robots and Systems*, 2016, pp. 279–285.
- [18] F. Blanchini, "Set invariance in control," *Automatica*, vol. 35, no. 11, pp. 1747 – 1767, 1999.
- [19] A. D. Ames, S. Coogan, M. Egerstedt, G. Notomista, K. Sreenath, and P. Tabuada, "Control barrier functions: Theory and applications," in *18th European Control Conference*, 2019, pp. 3420–3431.
- [20] R. Rajamani, *Vehicle Dynamics and Control*. Springer US, 2012.
- [21] J. Kong, M. Pfeiffer, G. Schildbach, and F. Borrelli, "Kinematic and dynamic vehicle models for autonomous driving control design," in *2015 IEEE Intelligent Vehicles Symposium (IV)*, 2015, pp. 1094–1099.
- [22] M. Santillo and M. Jankovic, "Collision free navigation with interacting, non-communicating obstacles," in *2021 American Control Conference (ACC)*, 2021, pp. 1637–1643.
- [23] M. Jankovic and M. Santillo, "Collision avoidance and liveness of multi-agent systems with cbf-based controllers," in *2021 60th IEEE Conference on Decision and Control (CDC)*, 2021, pp. 6822–6828.

APPENDIX I LQR-BASED NOMINAL CONTROL LAW

The nominal control inputs for each vehicle, ω_i^0 and $a_{r,i}^0$, were computed using LQR for trajectory tracking in the following way. For each vehicle, we assume that a desired state trajectory, $q_i^*(t) = [x_i^* \ y_i^* \ \dot{x}_i^* \ \dot{y}_i^*]^T$, is available. Then, we define the modified state vector and tracking error as $\zeta_i(t) = [x_i \ y_i \ \dot{x}_i \ \dot{y}_i]^T$, and $\tilde{\zeta}_i(t) = \zeta_i(t) - q_i^*(t)$ respectively. We then compute the optimal LQR gain, K , for a planar double integrator model and compute $\mu = [a_{x,i} \ a_{y,i}]^T = -K\tilde{\zeta}_i$. Then, we map $a_{x,i}, a_{y,i}$ to $\omega_i^0, a_{r,i}^0$ via

$$\begin{bmatrix} \omega_i^0 \\ a_{r,i}^0 \end{bmatrix} = S^{-1} \begin{bmatrix} a_{x,i} + \dot{y}_i \dot{\psi}_i \\ a_{y,i} - \dot{x}_i \dot{\psi}_i \end{bmatrix},$$

where

$$S = \begin{bmatrix} -v_{r,i} \sin(\psi_i) \sec^2(\beta_i) & \cos(\psi_i) - \sin(\psi_i) \tan(\beta_i) \\ v_{r,i} \cos(\psi_i) \sec^2(\beta_i) & \sin(\psi_i) + \cos(\psi_i) \tan(\beta_i) \end{bmatrix},$$

the inverse of which exists as long as $v_{r,i} \neq 0$. Therefore, if $|v_{r,i}| < \epsilon$, where $0 < \epsilon \ll 1$, we assign $\omega_i^0 = 0$ and $a_{r,i}^0 = \sqrt{a_{x,i}^2 + a_{y,i}^2}$.

- [8] M. Black, K. Garg, and D. Panagou, "A quadratic program based control synthesis under spatiotemporal constraints and non-vanishing disturbances," *59th IEEE Conf. on Decision and Control*, 2020.
- [9] A. Singletary, P. Nilsson, T. Gurriet, and A. D. Ames, "Online active

Proceedings of the 10th ACM/IEEE International Conf. on Cyber-Physical Systems, New York, NY, USA, 2019, p. 270–279.